

Disrupted Intrinsic Local Synchronization in Poststroke Aphasia

Mi Yang, MD, Jiao Li, MS, Dezhong Yao, PhD, and Huaifu Chen, PhD

Abstract: Evidence has accumulated from the task-related and task-free (i.e., resting state) studies that alternations of intrinsic neural networks exist in poststroke aphasia (PSA) patients. However, information is lacking on the changes in the local synchronization of spontaneous functional magnetic resonance imaging blood-oxygen level-dependent fluctuations in PSA at rest.

We investigated the altered intrinsic local synchronization using regional homogeneity (ReHo) on PSA (n = 17) and age- and sex-matched healthy controls (HCs) (n = 20). We examined the correlations between the abnormal ReHo values and the aphasia severity and language performance in PSA.

Compared with HCs, the PSA patients exhibited decreased intrinsic local synchronization in the right lingual gyrus, the left calcarine, the left cuneus, the left superior frontal gyrus (SFG), and the left medial of SFG. The local synchronization (ReHo value) in the left medial of SFG was positively correlated with aphasia severity ($r = 0.55$, $P = 0.027$) and the naming scores of Aphasia Battery of Chinese ($r = 0.66$, $P = 0.005$). This result is consistent with the important role of this value in language processing even in the resting state.

The pathogenesis of PSA may be attributed to abnormal intrinsic local synchronous in multiple brain regions.

(*Medicine* 95(11):e3101)

Editor: Richard Alan Rison.

Received: September 30, 2015; revised: February 11, 2016; accepted: February 25, 2016.

From the Center for Information in BioMedicine (MY, JL, DY, HC), Key Laboratory for Neuroinformation of Ministry of Education, School of Life Science and Technology, University of Electronic Science and Technology of China, and Department of Stomatology (MY), the Fourth People's Hospital of Chengdu, Chengdu, China.

Correspondence: Huaifu Chen, Center for Information in BioMedicine, Key Laboratory for NeuroInformation of Ministry of Education, School of Life Science and Technology, University of Electronic Science and Technology of China, Chengdu, China (e-mail: chenhf@uestc.edu.cn).

Financial disclosure: all authors have no financial relationships relevant to this article to disclose.

Data availability statement: data contain patient-identifying information and sharing is restricted by the ethics committee of the Fuzhou Hospital. Data request may be sent to the corresponding author.

Author contributions: DY and HC conceived and designed the experiments; MY, JL, and HC prepared the samples and analyzed the data; MY, JL, and HC participated in interpreting and analyzing the data; MY, JL, and HC wrote the paper.

Funding: the work is supported by the 973 project (2012CB517901), the 863 project (2015AA020505), the Natural Science Foundation of China (61533006 and 61125304) the Specialized Research Fund for the Doctoral Program of Higher Education of China (No. 20120185110028), and the Fundamental Research Funds for the Central Universities (ZYGX2013Z004).

The authors have no conflicts of interest to disclose.

Copyright © 2016 Wolters Kluwer Health, Inc. All rights reserved.

This is an open access article distributed under the Creative Commons Attribution-NonCommercial-NoDerivatives License 4.0, where it is permissible to download, share and reproduce the work in any medium, provided it is properly cited. The work cannot be changed in any way or used commercially.

ISSN: 0025-7974

DOI: 10.1097/MD.0000000000003101

Abbreviations: ABC = aphasia battery of Chinese, AQ = aphasia quotient, BOLD = blood-oxygen-level dependent, CQ = cortical quotient, fMRI = functional magnetic resonance imaging, KCC = Kendall's coefficient of concordance, PQ = performance quotient, PSA = post-stroke aphasia, ReHo = regional homogeneity.

INTRODUCTION

Poststroke aphasia (PSA) is a significant clinical problem that is usually caused by left hemisphere lesions.¹ Numerous functional neuroimaging are available for the investigation of the language architecture and the neurobiological mechanism underlying PSA.²

Glucose metabolism studies have shown that dominant hemisphere temporoparietal hypometabolism is responsible for language deficit and is related to the severity of aphasia.^{3,4} Functional magnetic resonance imaging (fMRI) signals that depend on the differential magnetic properties of oxygenated and deoxygenated hemoglobin are designated as the blood-oxygen-level dependent (BOLD) signal. The BOLD contrast mechanism directly reflects the neural responses elicited by a specific state, stimulus, or task.⁵ Task-related fMRI have most widely been used to map the (re)reorganization of language substrates in aphasia.⁶ Resting-state fMRI, in the absence of explicit stimulus, encodes physiologically meaningful indicators of the BOLD variation over time or over dynamic fluctuation of intrinsic brain activity, based on the fact that coherent low-frequency fluctuated BOLD signals widely exist in different but functionally related brain regions.^{7,8} In the resting state, dominant frontoparietal and default mode networks exhibit impaired remote regional functional connectivity in aphasia.^{9–12} Poststroke aphasia is assumed to produce language deficits by remote cortical and local cortical dysfunctions. The aberrance of intrinsic local synchronization in the brain would also be responsible for the effect of an individual cortical lesion.

Therefore, we utilized a regional homogeneity (ReHo) approach to examine the intrinsic local synchrony changes in aphasic patients. ReHo measures local synchronization in the spontaneous BOLD fluctuations of “nearest neighbor” voxels.¹³ Consequently, ReHo can feasibly be used to detect aberrance of brain intrinsic local synchrony.¹⁴ We hypothesized that aphasic patients at rest would show abnormal ReHo in certain regions. These abnormalities may be potential neuro-markers for aphasia patient diagnosis. Moreover, we further examined the correlations between the abnormal ReHo values and the aphasia severity and language performance for aphasia.

METHODS

Subjects

Seventeen PAS patients (all right-handed, 6 females; mean ± SD age, 53.53 ± 14.06 years old) were recruited from admission at the Fuzhou Hospital (see Table 1 for demographic information). Patients were recruited retrospectively according

TABLE 1. Demographics for Subjects

Demographics	Aphasia	Healthy Controls	P Value
Group size (n)	17	20	–
Handedness (left/right)	0/17	0/20	–
Gender (male/female)	11/6	12/8	0.90*
Age, y	53.53 ± 14.06	54.05 ± 8.43	0.98†
Education, y	8.71 ± 1.26	8.45 ± 1.47	0.58‡

Values are mean ± SD.
 * Chi-square test.
 † Mann Whitney U test.
 ‡ Two-sample t test.

to the following criteria: (i) first ever stroke occurred in the left hemisphere; (ii) age >18 and < 85 years; (iii) Chinese native speaker; (iv) aphasia persistent at day 1 poststroke; and (v) right handed. Participants were excluded if they had the following: (i) any past or current neurological disorders or family history of hereditary neurological disorders; (ii) a history of head injury resulting in loss of consciousness; (iii) alcohol or substance abuse; (iv) claustrophobia; and (v) incompatible implants. All patients experienced a single left hemisphere stroke (see Figure 1 for the lesion overlap map) and underwent MR imaging for an average of 9.9 ± 5.4 (± SD) days after stroke (see Table 2 for stroke-related clinical characteristics). All patients were Chinese native speakers and were right handed.

All patients received a comprehensive evaluation, including history and neurological examination, neuropsychological testing, and neuroimaging. Aphasia was diagnosed based on the Aphasia Battery of Chinese (ABC),¹⁵ which is the Chinese standardized adaptation of the Western Aphasia Battery.¹⁶ The ABC provides the aphasia quotient (AQ), performance quotient (PQ), and cortical quotient (CQ).¹⁷ The AQ reflects a global measure of aphasia severity and type of aphasia. The PQ represents the nonlinguistic function of the brain. The CQ gives an overall picture of cognitive status.¹⁸ Demographic and stroke-related clinical characteristics are shown in Table 2.

In total, 20 age-, gender-, and education-matched healthy controls (HCs) (all right-handed, 8 females, mean ± SD age, 54.05 ± 8.43 years old) were included in this study. The HCs were volunteers recruited through advertisement. These HCs had no history of neurological disorders or psychiatric illnesses and no gross abnormalities on brain MR images.

This study was approved by the local ethics Committee of the Fuzhou Hospital and was conducted in accordance with the

approved guidelines. All participants provided informed consent to participate in the investigation.

Data Acquisition

All data were analyzed using a 3.0T Siemens Vision Scanner (Erlangen, Germany) equipped with high-speed gradients on the recruitment day. The following parameters were axially used for T1 anatomical imaging: repetition time/echo time (TR/TE) = 2300/2.98 ms, matrix = 512 × 512, flip angle = 9°, voxel size = 0.5 × 0.5 × 1 mm³, and 176 slices without inter-slice gap. With the same locations as the anatomical slices, functional images were acquired using an echo-planar imaging sequence with the following parameters: TR/TE = 2000/30 ms, matrix = 64 × 64, flip angle = 90°, inter-slice gap = 4.0 mm, voxel size = 3.8 × 3.8 × 4 mm³, and slices = 31. Each participant underwent fMRI scan for 6 minutes, and 190 volumes were obtained. The participants were instructed to rest with their eyes closed, not to think of anything in particular, and not to fall asleep during scanning.

Data Preprocessing

Functional image preprocessing was performed using the Data Processing Assistant for Resting-State fMRI (DPARSF) (<http://www.restfmri.net>)¹⁹ and SPM8 tool kits (<http://www.fil.ion.ucl.ac.uk/spm>). We removed the first 10 functional volumes, because of the unstable signal and inability of the subjects to adapt. We adjusted the remaining images for temporal and spatial differences. We removed the functional image data with translation or rotation parameters that exceeded ± 1 mm or ± 1°. We also calculated individuals mean frame-wise displacement by the translation and rotation parameters of head motion according to the formula in

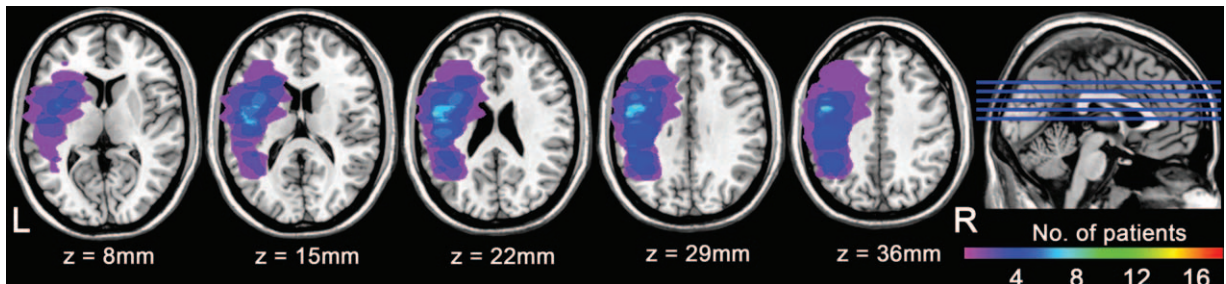


FIGURE 1. Distribution of the lesion areas of all patients. The lesion areas overlap across patients were rendered on the brain. Colors represent number of patients with a lesion to a specific voxel.

previously proposed issues.²⁰ No significant differences were found in the mean frame-wise displacement ($P = 0.16$) between groups. We then warped the functional images into a standard stereotaxic space at a $3 \times 3 \times 3 \text{ mm}^3$ resolution, using the Montreal Neurological Institute echo-planar imaging template. We removed linear trends from time courses and temporal band-pass filtering (0.01–0.08 Hz).

ReHo Analysis

We used Kendall’s coefficient of concordance (KCC) to measure the regional homogeneity, for the similarity of the time series within a functional cluster.¹³ We defined 27 nearest neighboring voxels as a functional cluster. The regional homogeneity of time series of the K voxels was calculated by the following equation:¹³

$$W = \frac{\sum_{i=1}^n (R_i)^2 - n(\bar{R})^2}{\frac{1}{12}K^2(n^3 - n)}$$

where W was the KCC among the K voxels, ranging from 0 to 1, $R_i = \sum_{j=1}^K r_{ij}$ was the sum rank of the i th time point, and r_{ij} was the rank of the j th voxel, i th time point. $\bar{R} = ((n + 1)K)/2$ was the mean of R_i ; K was the number of time series in a measured functional area ($K = 27$, the sum of given voxel and its 26 nearest voxels); n was the number of ranks ($n = 180$). We used the RESting-state fMRI data analysis Toolkit (REST) software (<http://sourceforge.net/projects/resting-fmri>) to calculate the time series of every voxel and its nearest voxels for regional homogeneity 1 by 1, to obtain the individual ReHo map. For further comparison within and between groups, the individual ReHo map was z score standardized. The ReHo value subtracts the mean from the value at each voxel and divides the value at each voxel by the standard deviation.^{14,21} Finally, the standardized ReHo maps were spatially smoothed with a 4-mm full-width Gaussian filter at half maximum.

Statistical Analysis

One-sample t test was performed for within-group comparison. We conducted individual standardized ReHo maps in each group to 1-sample t test. For visual inspection, ReHo patterns of each group were obtained by an uncorrected significant threshold.

To investigate differences in intrinsic local synchronization between aphasia patients and healthy controls, the 2-sample t test was performed on the individual standardized ReHo maps. We included age, gender, and education level as covariates. The significance threshold was set at a false discovery rate (FDR) corrected $P < 0.05$.

Finally, we used Pearson correlation to determine whether the abnormal ReHo regions are correlated with the clinical scores for ABC in aphasia patients. Based on the result of the 2-sample t tests, we exacted the mean z value of every patient in the region of interest, which was the abnormal region in aphasia. We then computed the Pearson correlation coefficient among these ReHo values and the clinical scores for ABC. As these analyses were exploratory, we used an uncorrected statistical significance level of $P < 0.05$.

RESULTS

Demographics and Clinical Characteristics

The PSA patients and HCs did not significantly differ in age (2 sample t test, $P = 0.98$), gender (chi-square test,

TABLE 2. Stroke-Related Clinical Characteristics for Patients

No	Gender	Age (Y)	Educ. (Y)	Aphasia Type	Type of Stroke	Site of Lesion	Size of Lesion (cm ³)	Initial Aphasia Severity	Time Poststroke (D)	Time CQ	Understanding	Repetition	Naming	Reading & Writing	Applying Structure		
1	M	51	10	Conduction	Ischemic	Frontal, limbic	119.22	40.6	14	10.1	35.7	106	100	17	43	12	
2	F	71	10	Conduction	Hemorrhagic	Frontal, parietal, insular	145.58	46.2	16	29.1	61.5	186	100	128	54	73	
3	M	33	9	Broca’s	Ischemic	Temporal, occipital	101.62	25.4	5	3.1	19.9	82	76	9	6	12	
4	M	44	8	Anomic	Ischemic	Frontal, parietal	70.38	60.6	16	33.7	74.0	200	100	156	60	80.5	
5	M	60	9	Anomic	Ischemic	Temporal, occipital	159.56	34.7	11	6.0	27.9	91	86	39	14	16	
6	F	47	9	Anomic	Ischemic	Frontal, insular	177.86	42.3	2	33.5	64.2	190	100	142.5	18	92.5	
7	M	63	8	Anomic	Ischemic	Temporal, occipital	68.57	53.2	5	28.2	63.9	183	100	66	56	81	
8	F	65	6	Anomic	Ischemic	Temporal, occipital	125.14	50.2	9	35.4	70.2	193	100	46	167	87	
9	F	77	10	Conduction	Ischemic	Subcortical, insular	75.80	32	7	18.2	39.7	110	92	12	72	40	43
10	M	54	7	Anomic	Ischemic	Temporal	48.74	51.8	17	30.5	66.3	198	95	60	135.5	56	76.5
11	M	37	7	Anomic	Ischemic	Temporal, occipital	46.86	61	3	35.0	75.5	200	100	96	177	60	72.5
12	M	69	9	Anomic	Ischemic	Frontal, temporal	1.68	57.4	15	36.4	74.3	184	100	86	172.5	60	91.5
13	M	38	9	Anomic	Hemorrhagic	Frontal, temporal, insular	122.78	27.7	17	15.9	34.2	89	90	3	68.5	24	50.5
14	F	57	8	Conduction	Ischemic	Temporal	32.15	37.2	8	16.9	35.5	101	85	0	44.5	42	54
15	M	64	11	Conduction	Ischemic	Frontal, temporal, limbic	20.01	34.2	14	18.6	41.7	121	88	19	63.5	46	45.5
16	M	51	10	Conduction	Ischemic	Temporal, occipital	225.77	2.5	3	12.7	30.0	96	74	2	37	42	20
17	F	29	9	Broca’s	Ischemic	Temporal, limbic	76.55	15.4	7	13.9	28.4	137	2	6	26	34	56

CQ = cortical quotient, Educ = education, F = female, M = male, PQ = performance quotient.

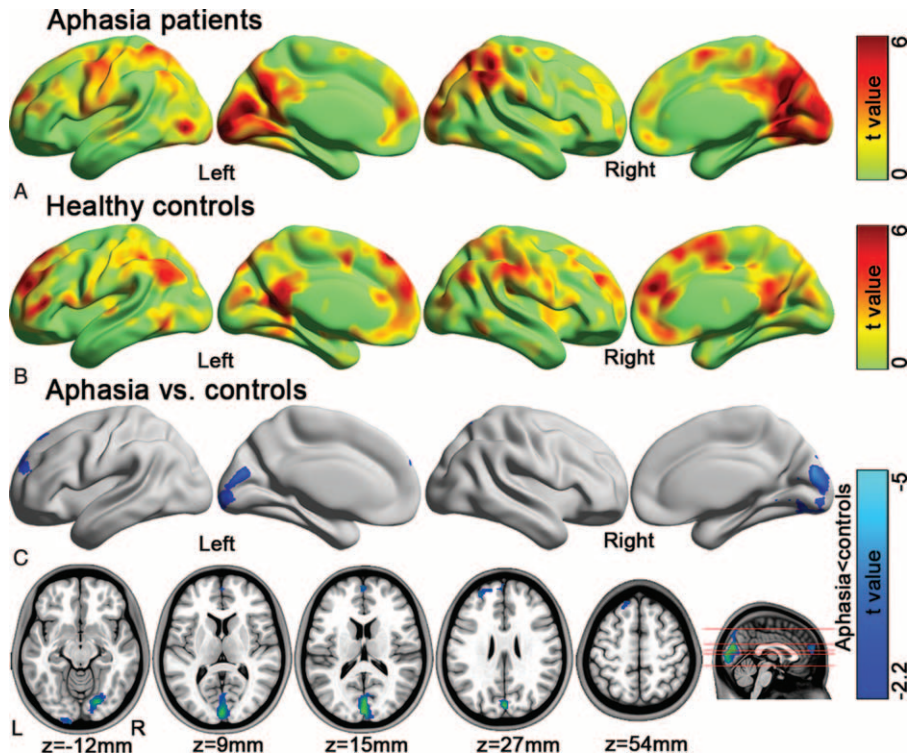


FIGURE 2. Comparison of intrinsic local synchronization patterns between groups. For visual inspection, ReHo maps of each group were obtained by uncorrected 1-sample *t* test (A for the aphasia patients group, and B for the healthy controls group). The results are presented on inflated surface maps by BrainNet Viewer (www.nitrc.org/projects/bnv). (C) The ReHo map of statistically significant differences between aphasia patients and HC by 2-sample *t* test ($P < 0.05$ FDR-corrected). The results are presented on inflated surface maps (*upper*) and axial maps (*lower*). Cold colors indicate ReHo decreases (aphasia<controls). Numbers below in each axial map refer to the z plane coordinates of the MNI space. Letters L and R correspond to the left and right sides of the brain, respectively. Further details of these regions are presented in Table 3. FDR=false discovery rate, HC=healthy controls, MNI= Montreal Neurological Institute, ReHo= regional homogeneity.

$P = 0.90$), and years of education (Mann–Whitney *U* test, $P = 0.58$) (Table 1). The scale score of patients included the following: understanding, repetition, naming, reading and writing, apply, structure, AQ, PQ, and CQ (Table 2). A manually drawn outline of the lesion on the T1 image of patients is illustrated in Figure 1.

ReHo Group Comparison

Within-group comparison of intrinsic local synchronization patterns, which are merely for visualizing, are shown in Figure 1 (1-sample *t* test, uncorrected for visual inspection). Visual inspection indicated that the posterior cingulate cortex/

precuneus, medial prefrontal cortex, and bilateral angular gyrus exhibited significantly higher ReHo than other brain regions, which were consistent with our previous study.²² The ReHo pattern was very similar to the so-called default mode network.²³ In addition, other brain regions, including the bilateral supplementary motor area, anterior cingulate gyrus, middle occipital gyrus, and cuneus and fusiform gyrus, have higher ReHo values.²²

Compared with HC, the PSA patients showed significantly decreased ReHo in right lingual gyrus, left calcarine, left cuneus, left superior frontal gyrus (SFG), and left medial SFG (SFGmed) ($P < 0.05$, FDR-corrected) (Figure 2 and Table 3).

TABLE 3. Brain Regions With Decreased ReHo in Aphasia Patients

Brain Region	MNI Coordinates (x, y, z) (mm)	T Value	Voxel Size
Right lingual gyrus	(18, -81, -12)	-4.21	66
Left calcarine	(0, -93, 12)	-4.96	195
Left cuneus	(0, -93, 15)	-5.07	76
Left superior frontal gyrus	(-15, 45, 48)	-3.80	29
Left medial superior frontal gyrus	(-3, 60, 21)	-3.80	55

x, y, z, coordinates of primary peak locations in the Montreal Neurological Institute (MNI) space.
 T value, statistical value of peak voxel showing ReHo differences between the groups.

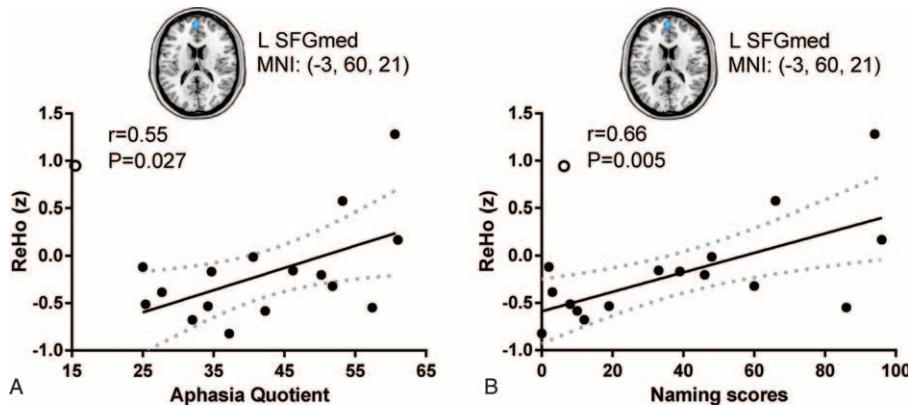


FIGURE 3. Correlations between the ReHo value in left medial of superior frontal gyrus and clinical characteristics. The ReHo value in left medial of superior frontal gyrus were positively correlated with correlated with AQ scores ($r=0.55$, $P=0.027$) and naming scores on ABC ($r=0.66$, $P=0.005$). Filled circles denote data points included in the correlation; open circles denote outliers. Solid line and dashed lines represent the best-fit line and 95% confidence interval of Pearson correlation, respectively. ABC=aphasia battery of Chinese, AQ=aphasia quotient, ReHo=regional homogeneity.

Correlations Between ReHo and Clinical Characteristics

The linear Pearson correlation between disturbed ReHo values and stroke-related clinical ABC scores in PSA patients was calculated. The ReHo value in left SFGmed was positively correlated with AQ scores ($r=0.55$, $P=0.027$) and naming scores on ABC ($r=0.66$, $P=0.005$) (Figure 3). We found no significant correlation between the others brain regions and local clinical symptoms’ ABC scores (Table 4).

DISCUSSION

To the best of our knowledge, this is the first resting-state fMRI to examine the disruption of intrinsic local synchronization (or local connectivity) in PSA patients. Aphasic patients exhibited significantly decreased local synchronization in the visual cortex associated with language and semantic processing and the anterior part of DMN than HCs. Furthermore, the correlation analyses revealed that the local synchronization

in the left SFGmed was positively correlated with naming score of ABC, indicating the impairment of production for language ability.

Decreased ReHo was also observed in the right lingual gyrus. The lingual gyrus is associated with language and semantic processing,²⁴ which is considered an essential element of human language. Previous task-related fMRI study demonstrated the activation of lingual gyrus in semantic and visual lexical decision task and silent reading.²⁵ Given that PSA is often accompanied by cognitive and expressive communication impairment and social communication barriers,²⁶ the decreased intrinsic local synchronization of lingual gyrus may contribute to the impairment of visual-spatial recognition, attention, working memory, and language expression. In addition, the patients with apraxia of speech exhibited abnormal lingual kinematics during consonant production and increasing word length.²⁷ The present findings suggest that lingual gyrus is closely related to normal integrative functions of language in aphasia not only during task, but also at rest.

TABLE 4. Association of ReHo With Clinical Scores in Aphasia Patients

Clinical Scores	Association With Brain Region [†] (r)				
	R. LING	L. CAL	L. CUN	L. SFG	L. SFGmed
Aphasia Quotient	-0.09	-0.20	-0.18	-0.08	0.55*
Performance Quotient	-0.06	-0.34	-0.35	0.01	0.30
Cortical quotient	-0.06	-0.29	-0.29	-0.04	0.42
Understanding	-0.06	-0.26	-0.27	-0.01	0.43
Repetition	-0.23	-0.34	-0.33	-0.41	0.37
Naming	0.11	0.06	0.10	0.01	0.66**
Reading and writing	-0.01	-0.29	-0.30	-0.06	0.30
Applying	-0.18	-0.38	-0.39	0.01	0.33
Structure	-0.02	-0.32	-0.33	0.17	0.20

CAL = calcarine, CUN = cuneus, L = left, LING = lingual gyrus, R = right, SFG = superior frontal gyrus, SFGmed = medial of superior frontal gyrus.

[†] Brain regions with ReHo reduction in aphasia patients.

* $P < 0.05$.

** $P < 0.01$.

Decreased ReHo in aphasic patients was also found in the left cuneus and calcarine [Brodmann's 18 (BA 18)]. Visual and auditory pathways are crucial to language and memory. The left calcarine was highly activated during processing of pseudo-words and real words.²⁸ Furthermore, decreased task-related brain activation in the left calcarine is found in dyslexic patients, indicating reading disability in the semantic system.²⁹ In addition, word condition could activate the cuneus, which is associated with auditory processing.³⁰ These data, along with the present findings, suggest that the left cuneus and calcarine (BA 18) are closely related to language and semantic processing in aphasia.

Local synchronization was significantly decreased in the left SFG, which is considered as a key region in the language network.³¹ Aphasic patients showed a significantly decreased intrinsic remote FC in bilateral SFG and medial frontal gyrus.¹¹ As for the language area, the gray matter and fractional anisotropy of SFG were lost in PSA.³² The SFG was also thought to be included in the salience network, which was an important system in cognitive control and an essential factor in PSA recovery.³³ According to these previous studies and the present findings, the left SFG plays an important role in aphasia.

Compared with the HCs, aphasic patients showed decreased local synchronization in the left SFGmed, which was a key hub of DMN.²³ In addition, a significant positive correlation was found between the ReHo of the left SFGmed and naming score on ABC in the aphasia group. Damage in the SFGmed was related to the impairment on phonemic verbal fluency and speech in aphasic patients.³⁴ Moreover, the medial frontal area was thought to be associated with automatic propositional speech, semantic variant, and word generation in primary progressive aphasia.³⁵ Aphasic patients showed abnormal FC in the medial frontal in DMN, which likely plays a crucial role in motor aphasia.¹¹ In a recent study, transcortical motor aphasia, characterized by comprehension, intact repetition, and object naming, was associated with the damage to the left medial frontal area.³⁴ Furthermore, medial frontal cortex was functionally connected to the inferior parietal lobe, which is a key region in language processing by remote regional FC.³⁶ In addition to remote dysfunction, the current finding of intrinsic local dysfunction may provide new insights into how the medial of superior frontal areas affect the language system in PSA patients. The role of left SFGmed in language response may partially contribute to the pathogenesis of aphasia.

This study has several methodological limitations. First, the sample size is relatively small for conduction steady evidence for abnormal local synchronization in aphasia. Second, the healthy subjects were not tested with ABC for language performance. In addition, a longitudinal study is needed to examine whether the pretreatment intrinsic local synchronization would serve as a predictor for prognosis of recovery of aphasia following anomia treatments. The resting-state functional connectivity has been used for prognosis of recovery of aphasia.² Finally, constructing functional connectome will provide new ways of conceptualizing the mechanisms of aphasia.

In summary, patterns of intrinsic local synchronization are altered in PSA patients at rest. These patients exhibit significantly decreased local synchronization in the visual cortex, which is associated with language and semantic processing in the anterior part of DMN linked to language comprehension. Furthermore, the local synchronization in left SFGmed is associated with aphasia severity and naming score of ABC, thereby indicating the impairment of production for language ability. These results from local neural dysfunction may provide

a novel way of investigating the neuro-pathophysiological PSA mechanisms.

ACKNOWLEDGMENTS

The author thanks the First Affiliated Hospital of Fujian Medical University for Data acquisition.

REFERENCES

- Damasio AR. Aphasia. *N Engl J Med*. 1992;326:531–539.
- Crinion JT, Leff AP. Using functional imaging to understand therapeutic effects in poststroke aphasia. *Curr Opin Neurol*. 2015;28:330–337.
- Karbe H, Herholz K, Szeliess B, et al. Regional metabolic correlates of Token test results in cortical and subcortical left hemispheric infarction. *Neurology*. 1989;39:1083–1088.
- Metter EJ, Hanson WR, Jackson CA, et al. Temporoparietal cortex in aphasia. Evidence from positron emission tomography. *Arch Neurol*. 1990;47:1235–1238.
- Logothetis NK. The neural basis of the blood-oxygen-level-dependent functional magnetic resonance imaging signal. *Philos Trans R Soc Lond B Biol Sci*. 2002;357:1003–1037.
- Crosson B, McGregor K, Gopinath KS, et al. Functional MRI of language in aphasia: a review of the literature and the methodological challenges. *Neuropsychol Rev*. 2007;17:157–177.
- Fox MD, Raichle ME. Spontaneous fluctuations in brain activity observed with functional magnetic resonance imaging. *Nat Rev Neurosci*. 2007;8:700–711.
- Biswal B, Yetkin FZ, Haughton VM, et al. Functional connectivity in the motor cortex of resting human brain using echo-planar MRI. *Magn Reson Med*. 1995;34:537–541.
- Zhu D, Chang J, Freeman S, et al. Changes of functional connectivity in the left frontoparietal network following aphasic stroke. *Front Behav Neurosci*. 2014;8:167.
- Li R, Wang S, Zhu L, et al. Aberrant functional connectivity of resting state networks in transient ischemic attack. *PLoS One*. 2013;8:e71009.
- Wang X, Wang M, Wang W, et al. Resting state brain default network in patients with motor aphasia resulting from cerebral infarction. *Chin Sci Bull*. 2014;59:4069–4076.
- Marcotte K, Perlberg V, Marrelec G, et al. Default-mode network functional connectivity in aphasia: therapy-induced neuroplasticity. *Brain Lang*. 2013;124:45–55.
- Zang Y, Jiang T, Lu Y, et al. Regional homogeneity approach to fMRI data analysis. *Neuroimage*. 2004;22:394–400.
- Zuo XN, Xu T, Jiang L, et al. Toward reliable characterization of functional homogeneity in the human brain: preprocessing, scan duration, imaging resolution and computational space. *Neuroimage*. 2013;65:374–386.
- Gao SR, Chu YF, Shi S, et al. A standardization research of the aphasia battery of Chinese. *Chinese Mental Health Journal [Chinese]*. 1992;6:125–128.
- Lu J, Wu J, Yao C, et al. Awake language mapping and 3-Tesla intraoperative MRI-guided volumetric resection for gliomas in language areas. *J Clin Neurosci*. 2013;20:1280–1287.
- Liu L, Luo XG, Dy CL, et al. Characteristics of language impairment in Parkinson's disease and its influencing factors. *Transl Neurodegener*. 2015;4:2.
- Yu ZZ, Jiang SJ, Bi S, et al. Relationship between linguistic functions and cognitive functions in a clinical study of Chinese patients with post-stroke aphasia. *Chin Med J (Engl)*. 2013;126:1252–1256.

19. Chao-Gan Y, Yu-Feng Z. DPARSF: a MATLAB toolbox for “pipeline” data analysis of resting-state fMRI. *Front Syst Neurosci.* 2010;4:13.
20. Power JD, Barnes KA, Snyder AZ, et al. Spurious but systematic correlations in functional connectivity MRI networks arise from subject motion. *Neuroimage.* 2012;59:2142–2154.
21. Yan CG, Craddock RC, Zuo XN, et al. Standardizing the intrinsic brain: towards robust measurement of inter-individual variation in 1000 functional connectomes. *Neuroimage.* 2013;80:246–262.
22. Qiu C, Liao W, Ding J, et al. Regional homogeneity changes in social anxiety disorder: a resting-state fMRI study. *Psychiat Res-Neuroim.* 2011;194:47–53.
23. Raichle ME, MacLeod AM, Snyder AZ, et al. A default mode of brain function. *Proc Natl Acad Sci U S A.* 2001;98:676–682.
24. Heath S, McMahon KL, Nickels L, et al. Neural mechanisms underlying the facilitation of naming in aphasia using a semantic task: an fMRI study. *BMC Neurosci.* 2012;13:98.
25. Hart J Jr, Kraut MA, Kremen S, et al. Neural substrates of orthographic lexical access as demonstrated by functional brain imaging. *Neuropsychiatry Neuropsychol Behav Neurol.* 2000;13:1–7.
26. Lee B, Pyun SB. Characteristics of cognitive impairment in patients with post-stroke aphasia. *Ann Rehabil Med.* 2014;38:759–765.
27. Bartle-Meyer CJ, Goozee JV, Murdoch BE. Kinematic investigation of lingual movement in words of increasing length in acquired apraxia of speech. *Clin Linguist Phon.* 2009;23:93–121.
28. Xiao Z, Zhang JX, Wang X, et al. Differential activity in left inferior frontal gyrus for pseudowords and real words: an event-related fMRI study on auditory lexical decision. *Hum Brain Mapp.* 2005;25:212–221.
29. Liu L, Wang W, You W, et al. Similar alterations in brain function for phonological and semantic processing to visual characters in Chinese dyslexia. *Neuropsychologia.* 2012;50:2224–2232.
30. Rama P, Relander-Syrjanen K, Carlson S, et al. Attention and semantic processing during speech: an fMRI study. *Brain Lang.* 2012;122:114–119.
31. Nair VA, Young BM, La C, et al. Functional connectivity changes in the language network during stroke recovery. *Ann Clin Transl Neurol.* 2015;2:185–195.
32. Allendorfer JB, Storrs JM, Szaflarski JP. Changes in white matter integrity follow excitatory rTMS treatment of post-stroke aphasia. *Restor Neurol Neurosci.* 2012;30:103–113.
33. Brownsett SL, Warren JE, Geranmayeh F, et al. Cognitive control and its impact on recovery from aphasic stroke. *Brain.* 2014;137:242–254.
34. Chapados C, Petrides M. Impairment only on the fluency subtest of the Frontal Assessment Battery after prefrontal lesions. *Brain.* 2013;136:2966–2978.
35. Agosta F, Galantucci S, Valsasina P, et al. Disrupted brain connectome in semantic variant of primary progressive aphasia. *Neurobiol Aging.* 2014;35:2646–2655.
36. Yeo BT, Krienen FM, Sepulcre J, et al. The organization of the human cerebral cortex estimated by intrinsic functional connectivity. *J Neurophysiol.* 2011;106:1125–1165.